# NASA Technical Memorandum 81805



# DEVELOPMENT OF TEST METHODS FOR SCALE MODEL SIMULATION OF AERIAL APPLICATIONS IN THE NASA LANGLEY VORTEX RESEARCH FACILITY



Frank L. Jordan, Jr.

April 1980

National Aeronautics and
Space Administration

**Langley Research Center**
Hampton, Virginia 23665

# DEVELOPMENT OF TEST METHODS FOR SCALE MODEL SIMULATION OF AERIAL APPLICATIONS IN THE NASA LANGLEY VORTEX RESEARCH FACILITY

Frank L. Jordan, Jr.
NASA Langley Research Center
Hampton, Virginia 23665

## Abstract

The Langley Research Center of the National Aeronautics and Space Administration is currently engaged in basic research to improve aerial applications technology. As a key part of this program, methods have been developed at the Langley Vortex Research Facility to simulate and measure deposition patterns of aerially-applied sprays and granular materials by means of tests with small-scale models of agricultural aircraft and dynamically-scaled test particles. Interactions between the aircraft wake and the dispersed particles are being studied with the objective of modifying wake characteristics and dispersal techniques to increase swath width, improve deposition pattern uniformity, and minimize drift. This paper describes the particle scaling analysis, test methods for particle dispersal from the model aircraft, visualization of particle trajectories, and measurement and computer analysis of test deposition patterns. An experimental validation of the scaling analysis and test results that indicate improved control of chemical drift by use of winglets, are presented to demonstrate test methods.

## Introduction

Since 1976 the National Aeronautics and Space Administration has been engaged in basic research to improve aerial applications technology. Two problem areas recognized in this program as being important to aerial applicators are obtaining a suitable deposition pattern (single-swath concentration of material on the ground), and controlling drift of toxic chemicals from the target crop. Ideally, a deposition pattern is desired which will result in a uniform concentration of material on the crop, with a minimum number of passes over the field -- that is, with the maximum spacing between adjacent swaths. In actual practice, nonuniformity of coverage on crops and drift results in a large loss in productivity in terms of chemical waste and an associated environmental or health hazard.

With aerial sprays, a major factor that affects both the shape of the deposition pattern and the drift problem is the interaction of the aircraft wake with the spray drops. An example of spray-wake interaction, illustrating primarily undesirable effects, is shown in the photograph in Figure 1.*. Principal regions where undesirable interactions occur are in the wing-tip vortex flow, where small drops are entrained and remain airborne, becoming more susceptible to drift; and in the propeller slipstream, where drops are given a lateral bias. Typical effects of these interactions on the deposition pattern are illustrated in Figure 2, which shows a comparison between ideal and actual patterns. The trapezoidal pattern (dotted line) is desirable because the sloping sides of the pattern overlap on adjacent swaths, permitting some variation in lateral swath accuracy (spacing) without significant degradation in uniformity of coverage. Large differences are apparent between ideal and actual patterns as illustrated in Figure 2, in terms of both total deposit and pattern shape. The amount of chemical deposit in the swath is often considerably less than the amount applied, and the pattern shape is not uniform but contains regions of both over- and under-concentration of chemicals. For medium sprays (300-400 microns Volume Median Diameter), for instance, only 70 percent of the applied chemical may be recovered within 305 meters (1000 ft.) downwind of the flight path even with relatively low altitude application (material released under 3.05 meters height) under low-wind conditions (5-8 Km/hr)(ref.1). Interaction of the aircraft wake with the dispersed spray, therefore, seriously degrades overall application system performance by increasing the potential for drift and decreasing the quality of coverage. On the other hand, it is important to recognize that the spanwise flow in the vortex is a desirable transport mechanism for the larger drops, in that it increases swath width.

With the aerial spreading of dry materials such as seeds, fertilizer, and granular pesticides, it does not appear that the wake flow fields of conventional agricultural aircraft significantly affect deposition patterns. Agricultural granulars are large (sizes range from 500 to 3500 microns) and are distributed from spreaders that are normally located under the aircraft fuselage, away from wingtip vortex flows. A recent analytical study (ref. 2), however, has indicated that it may be possible to achieve significant lateral transport of these large particles and increase swath width by use of high lift devices positioned to create a strong vortex near the location of particle release.

Early in the NASA Aerial Applications Program, it was recognized that test methods were needed to simulate aerial dispersal of materials under controlled conditions that would permit study of the various factors which affect deposition. Thus, at the Langley Vortex Research Facility, test methods have been developed over the past three years to simulate and measure deposition patterns of aerially-applied sprays and granular materials by means of tests with small-scale models of agricultural aircraft and dynamically-scaled test particles. A status report on early development activities was published in 1978 (ref. 3). The purpose of this paper is to update this earlier work by providing a description of the more recent developments at the Vortex Facility, including refinements in the overall test methods and examples of test results.

## Symbols

| | |
|---|---|
| b | wing span |
| C | particle mass concentration across the swath |
| $C_D$ | drag coefficient of the particle |
| d | propeller diameter |

*Photograph courtesy of World of Agricultural Aviation Magazine

| | |
|---|---|
| $d\delta/dy_G$ | variation of particle diameter across the deposit width |
| $dv/d\delta$ | variation of mass Q across the diameter spectrum |
| g | acceleration due to gravity |
| h | height above ground plane |
| n | propeller rotational speed |
| Q | mass per release point per semispan along the flight path |
| Re | Reynold's No. of the particle |
| t | time |
| $U_\infty$ | airplane or free-stream velocity |
| v | percent of total mass |
| $V_G$ | spanwise location of particle deposit |
| $\Gamma$ | total circulation of wing |
| $\Gamma_p$ | total circulation of propeller |
| $\delta$ | particle diameter |
| $\Theta_p$ | angular propeller position |
| $\mu$ | absolute air viscosity |
| $\rho$ | air density |
| $\sigma$ | particle density |

## Objectives and Approach

The ultimate objective of this research is to determine how to integrate airplane wake characteristics with dispersal techniques in such a manner as to improve overall application system performance in terms of producing wide, uniform deposition patterns with a minimum of material lost from the target area due to drift. The research efforts to date have been directed mainly toward developing and validating the required experimental and theoretical research tools necessary for scale-model simulation of aerial applications under controlled test conditions.

The principal objectives of this early activity are: first, to develop methods to simulate aerial dispersal; second, to develop a data base to quantify wake and dispersal characteristics; and finally, to examine wake modification as a method of producing favorable changes in deposition characteristics.

Aerodynamic wake modification is believed to be a means by which wake-dispersal interactions may be improved. The objective of wake modification is to minimize undesirable effects of wake flow such as the entrainment of fine spray droplets in the wing tip vortex, while maximizing desirable effects, such as lateral transport of relatively large particles, liquid or granular (seed and fertilizer), which increases deposition pattern width. Technology developed through the NASA Wake Vortex Minimization Program for large jet transport aircraft is drawn upon to guide studies to identify candidate concepts for wake modification. Concepts found to be promising from scale-model tests in the Vortex Facility, and numerical simulations, are validated by correlation with full-scale tests, both in wind tunnels and in flight. Throughout this development, candidate concepts are evaluated to determine their effects on airplane performance, stability and control, in order to determine flight-worthiness and practicality. Concepts include both practical devices for retrofit to existing aircraft and new design considerations for future aircraft.

## Facility and Test Measurements

### Facility

The Vortex Facility, shown in the sketch in Figure 3, was used during the 1940's and 50's as a water-filled towing tank and impact basin to study stability, control, and performance of seaplanes and ditching characteristics of landplanes. During the past decade, the facility was converted to study the upset hazard associated with the strong wake vortices generated by large jet transport aircraft. In October 1976, the facility was further modified to permit testing of models of agricultural aircraft in ground effect.

One unique feature of this facility is that the test airplane model is moved through a stationary medium (air) rather than being held stationary while the test medium is forced by it as in conventional wind tunnels. This feature is essential to the study of ground deposition patterns behind model agricultural aircraft, and also permits observation of the model-generated wake for large distances behind, or downstream from the models.

The facility is 550 meters long and has an enclosed overhead track extending the length of the building. The wake generating airplane model is blade mounted on a strain-gage balance beneath a streamlined powered carriage, which travels along the overhead track. The support blade is adjustable to permit variation in model altitude and pitch. The model aircraft is towed at constant velocity through a test section enclosure which serves to isolate the carriage wake from the model. Test measurements are taken as the model passes over a ground plane installed in the test section. The test section is 91 meters long, 5.5 meters wide, and 5.2 meters high with a 5-cm wide opening in the ceiling to allow the model support blade to pass. The overhead track extends 305 meters ahead of the entrance to the covered area to permit the carriage to accelerate to test velocities up to 30 m/sec.

### Model Wake

Wake-vortex systems generated by the model airplanes are studied with flow-visualization and laser-doppler velocimetry. The flow visualization technique, which was developed at the facility, has proven quite suitable for obtaining time histories of wake development and decay. A screen of kerosene smoke, generally confined to a plane perpendicular to the model flight path, is injected into the facility test section and allowed to become stationary. The model is then propelled through the smoke and the wake action, made visible by the smoke induced along the flow streamlines, is recorded photographically with high-speed cameras. A detailed description of this flow visualization technique can be found in Reference 4.

Use of this technique for qualitative studies is demonstrated in Figure 4 which shows a photographic time sequence of development of the wake vortex system in ground effect behind a low-wing monoplane model. The upper-left photograph was taken before the model reached the smoke curtain, the upper-right photograph immediately after the model had passed through the smoke (the wing-tip vortex can be seen rolling up behind the left wing), and the lower photographs were taken at later stages

of vortex development as the model passed out of the test section. As seen, the wake quickly rolls up into a single vortex from each wing tip, each vortex being characterized by highly swirling flow near the vortex core. It is this swirling flow, of course, which causes the entrainment and subsequent drift of spray droplets.

Some recent refinements to the smoke ejection system and lighting have improved the quality of this photographic data. In early stages of system development smoke was ejected from two commercial smoke guns, one mounted on each test section wall, and illuminated from the front. With this arrangement, control of amount and distribution of smoke was difficult and frequently repeated test runs were necessary to obtain acceptable flow visualization. Currently, smoke is contained in plenum chambers and ejected through spanwise rows of small holes in the test-section ground plane (Figure 4, upper left photograph). Also, in current practice the smoke is illuminated from the back by lights beamed through windows in the ground plane.

The flow-visualization technique is also used for quantitative wake studies. Vortex trajectories are obtained by plotting the time variation of vortex-core position, as determined from photographs similar to those in Figure 4, as a function of distance behind the aircraft. Use of such quantitative data in the analysis of model size constraints for tests in the facility will be discussed later in this paper.

Wake characteristics are also studied quantitatively with a recently developed rapid-scan two-dimensional laser-doppler velocimeter (LDV). The LDV is capable of simultaneously measuring both vertical and axial (along flight path) velocity components in a near or far-field wake-vortex system. Its applicability to wake studies for agricultural airplanes, where vortex systems are often rapidly transporting in ground effect, has recently been demonstrated (ref. 5).

The technique utilizes an unique optical scanning system (ref. 6) which permits rapid incremental scanning of the laser focus point over the measurement region up to 30 times a second. As the vortex moves down and across the ground plane, it crosses the laser optical axis in the measurement region. Vertical velocity measurements through the vortex core (which measure the maximum tangential or swirl velocities in the vortex) are obtained as the vortex crosses the optical axis. Although originally designed to operate in the back-scatter mode, this system has recently been modified to forward-scatter operation. This refinement has greatly improved the sensitivity of the system. Velocity measurements in the vortex core, previously impossible with the old back-scatter mode, are now routine. The sketch in Figure 5 illustrates the relation of the laser beams to the vortex and presents a representative vertical velocity profile through the vortex core. The laser is beamed horizontally across the test section perpendicular to the model flight path. In the velocity profile persented, vertical velocity, U, normalized with respect to the airplane test flight speed $U_\infty$, is given as a function of spanwise distance, y, from the wing tip in semispans. As seen in Figure 5 maximum flow velocities near the vortex core are about thirty percent of flight speed. Such velocities are large compared to settling (terminal) velocities of small droplets in air. For instance, the settling velocity of 250-micron size water droplets is only about 1 m/sec in still air compared to maximum vortex swirl velocities of about 13 m/sec for a typical flight speed of 45 m/sec (100 miles/hr.). It is understandable how behavior of even large droplets sprayed from nozzles near the wing tip can be dominated by vortex flow dynamics and how vortex entrainment can be the inevitable fate of smaller droplets.

## Scaled Test Particles

Scaled test particles are dispersed from the model aircraft during test runs as the models pass over the ground plane. Closely graded glass or fillite spheres are contained in small hoppers (cylindrical containers) installed at different spanwise stations in the model wings, and gravity feed to ejectors (dispersal tubes) located in the wing lower surface (Figure 6). The ejectors are not intended to simulate full-scale nozzles; their purpose is to release particles in the model wake at a point which is out of the wing boundary-layer, introducing as little interference as possible. Particles can be ejected from a wide range of dispersal points, including spanwise, chordwise, and vertical positions. A "light curtain" perpendicular to the model flight path illuminates particles in the model wake, and particle trajectories are recorded by streak photography. Single-ejector deposition patterns are measured by collecting particles on adhesive-surfaced strips at spanwise sample regions at stations along the model flight path and then expressing particle concentration as a function of lateral distance from the flight path.

# Recent Improvements in Test Capability

## Scaling of Particle Trajectories

In order to permit results of scale-model tests to be extrapolated to full-scale conditions, scaling laws have been derived for the trajectories of particles released in the wakes of agricultural aircraft. These scaling parameters establish test similitude for dispersal of dynamically-scaled test particles from the model airplanes. Initially, scale parameters were derived for trajectories of liquid droplets (ref. 7). This analysis applies to droplets in the 100-to 500-micron diameter size range. Such droplets are nearly spherical in shape, permitting the classical drag variations for spheres to be used. It should be noted that since the scaling analysis as developed is only concerned with scaling the trajectory of a single particle, interference between particles is ignored.

The analysis concludes that to insure the same non-dimensional particle trajectory in the wake of a geometrically-scaled aircraft model, the following parameters must be held constant between the full-scale airplane and the model:

$$\frac{U_\infty^2}{bg}, \frac{\Gamma}{U_\infty b}, \frac{U_\infty t}{b}, \frac{h}{b}, \frac{\Gamma}{\Gamma_p}, \frac{U_\infty}{nd}, \frac{d}{b}, \Theta_p,$$

$$\frac{\rho^{1+\gamma}\,\delta^{\gamma-1}\,U_\infty^{2+\gamma}}{\sigma g \mu^{\gamma}} \qquad \text{(eq. 15, ref. 7).}$$

The first term indicated on the previous page is the square of the Froude number, which establishes model test velocity. The second parameter is nondimensional vortex strength, which determines model lift. The third term represents nondimensional time, and the fourth term is nondimensional height of model above the ground plane. The fifth through eighth terms deal with scaling of the propeller slipstream. Parameters are ratio of wing-to-propeller vortex strength, advance ratio, geometrical scale of propeller in terms of diameter, and angular orientation of the propeller when the particle is introduced into the flow. The last term shown establishes the relationship between the size and density of the scaled particles and results from the introduction of the particle drag curve as approximated by $C_D = BR_e^{\gamma}$, where $B$ and $\gamma$ are constants that are determined for the range of particle Reynolds numbers of interest.

Granular Particles.- Recently, the scaling analysis has been applied to dry granular particles such as agricultural seeds, fertilizer and granular pesticides (ref. 8). Seeds that were selected for scaling because of their economic importance included wheat, rice, oats, alfalfa, clover, sudan grass, and soybeans. Both granular and prilled fertilizer (spherical pellets) were scaled because of their obvious economic importance. Finally, to include the granular pesticides 16/30 and 30/60 graded clay attapulgate were scaled. The larger 16/30 clay is a popular carrier for granular pesticides such as herbicides for aquatic weed control. The small 30/60 clay, more drift prone, is used for herbicides and insecticides applied above the ground.

As mentioned previously, an assumption of the particle scaling laws is that the particle to be scaled is spherical. Because most agricultural granulars are non-spherical it was necessary to mathematically equate these particles to spheres possessing the same aerodynamic properties in order to utilize the scaling analysis. First, physical properties of the selected granulars were obtained from an extensive review of the literature. These properties included size, shape, density, and in most cases measured terminal velocities. Although the terminal velocity of a particle represents only one point on the drag coefficient versus Reynolds number curve, it has been widely accepted as the single most important aerodynamic property identifying the particle. Minimum, average, and maximum values of these properties were obtained, and for the seeds a number of different varieties were considered (seven different varieties of wheat, for instance). For scaling, aerodynamically similar spheres were determined by the "sphericity" approach. This scheme involves determining the non-spherical particle's volume and surface area, calculating the diameter and surface area of an equivalent volume sphere and then calculating a sphericity constant from the ratio of surface areas of sphere to non-spherical particle. This constant is a measure of how far the particle deviates from a true sphere, and is used with a family of particle $C_D$ versue $Re$ curves for different sphericities, established by early investigators. The particle diameter and drag coefficient obtained by the sphericity scheme was then used in Lapple's equation for the terminal velocity of a sphere. This calculated terminal velocity was compared with the measured terminal velocity of the non-spherical granular and an iterative procedure devised which used the measured terminal velocity along with Lapple's equation and the actual $C_D$ versus $Re$ curve for the granular particle in question to obtain a more exact value of particle diameter to be used in the scaling analysis. Agricultural granulars are not uniform in size or shape, of course, and therefore a range of diameters of equivalent spheres was determined for each type of particle.

The scaling analysis has been used to obtain a one-tenth scaling of all of the selected granular particles for use in tests with a 1/10-scale model of a representative low-wing agricultural monoplane. Shown as an example, Figure 7 is a plot of the scaled particle characteristics for wheat. Each curve of scaled particle diameter versus scaled particle density represents the range of allowable combinations of these two particle characteristics that scale to a single full-scale wheat seed. For instance, reading from the curve corresponding to the mean-sized seed, either a 1.0 millimeter particle with a density of 0.75 grams/cm$^3$ or a 0.5 millimeter particle with a density of 2.0 grams/cm$^3$ would be a valid scaling for the mean-sized wheat seed. These plots show scaled mean diameter, scaled representative range and total range. The mean diameter corresponds to the mean of all varieties found in the literature, the representative range corresponds to the range of a particular seed variety chosen to represent the average of all varieties, and the total range corresponds to the total range of all varieties from all investigators published. The small circles superimposed on each plot represent one commercial supplier's glass spheres which closely approximate the scaled diameters.

Experimental Validation.- Once the scaling analysis was completed, a test program was initiated to experimentally validate the particle scaling laws. First, a preliminary validation of the scaling was conducted (ref. 7) in which deposition patterns using two types of test particles, polystyrene and glass (which differ greatly in their physical characteristics), were compared. Polystyrene and glass particles were sized by the scaling laws to represent the same full-scale water droplet, and were released into the wake of a model airplane from single ejectors in separate test runs. This comparison showed very good agreement between these single-ejector depositions using the two types of particles, giving a preliminary validation of the scaling. Since the validation did not include comparisons between airplane models of different scales, and since full-scale depositions were not available for comparisons, only the particle-dynamics scaling was validated in these tests.

Recently, a more complete validation which includes a verification of aircraft-wake scaling as well as particle dynamics, has been conducted (ref. 9). Since full-scale data were not available for comparison it was necessary for the test to be self contained. In these tests results are compared between geometrically similar models of different scale. While most of the tests were conducted with the models unpowered, a limited test series was also conducted with an operational propeller to validate the scaling of the propeller slipstream effects.

The three models used in the unpowered-baseline scaling validation are shown in the photograph in Figure 8. Test conditions and particle characteristics were established by the scaling laws and single-ejector depositions were compared between the three models. The primary test objective was to scale the test particles for each model to represent a common full-scale water droplet and obtain agreement between the single-ejector depositions. An additional objective of this particular test series, however, was to establish model-size constraints imposed by adverse effects of the test-section walls on wake and deposition data. The three models represent scaling ratios of 0.10, 0.15, and 0.20 relative to a hypothetical full-scale aircraft having a wing span of 12.2 m (40 ft.), resulting in model spans of 1.22 m (4 ft.), 1.83 m (6 ft.), and 2.44 m (8 ft.). Since the wing and fuselage are the major aircraft components that influence particle trajectories, it was not believed essential to the scaling validation to include empennage components, and the models consisted only of wing-fuselage combinations. Commercially available glass sphere microbeads were found to best suit the requirements of this test. The glass microbeads were scaled for a full-scale water droplet having a diameter of approximately 490 microns, resulting in the following characteristics:

| Model Scale | Particle Diameter (microns) | Particle Density ($g/cm^3$) |
|---|---|---|
| 0.10 | 105 | 2.42 |
| 0.15 | 125 | 2.42 |
| 0.20 | 105 | 3.99 |

For this baseline scaling the model height was 0.51 semispans and lift coefficient was 0.61. Particles were collected on narrow adhesive strips placed spanwise on the test-section floor, and particle concentrations were expressed as percent of total deposit and plotted as a function of lateral distance, in semispans, from flight path. Data were obtained for spanwise ejector locations of 0.2 to 0.7 semispans in 0.1 semispan increments. The lateral position of the median of each single-ejector deposition was calculated and taken as the position the average particle would deposit.

Particle trajectories and median ground-deposition points from each ejector are shown in Figure 9. As can be seen, particles ejected outboard of the 0.25 semispan station are transported outward by the wing-tip vortex system, while particles ejected inboard of the 0.25 semispan station are transported inward by the wing-fuselage vortex. A particle ejected near the 0.25 semispan location, for this case, would not be transported laterally at all, but would fall directly downward to its deposition point. The lateral distance that the particle deposit is displaced from the ejector, as dimensioned on this figure, is an important measure of the influence of the wake-vortex system on the particle.

The baseline scaling-law validation is presented in Figure 10 as a comparison between the lateral displacement of the median of the particle deposit from each ejector, as a function of ejector location, for each of the three models. The physical interpretation of these data is that a particle ejected from the 0.4 semispan ejector position, for example, is transported approximately 0.2 semispans outboard. The point where the curve crosses the horizontal axis, at about 0.25 semispans, corresponds to the point at which no lateral transport of the particle occurs. Points above the horizontal axis indicate particle transport outboard, whereas points below indicate particle transport inboard.

The validity of the scaling laws is indicated in this figure by the excellent agreement shown between the data collected for the different model scales. Based on the close agreement between these cases, the experimental non-dimensional median deposition points from scale-model tests should accurately correspond to those of the full-scale case.

Figure 11 compares the actual deposition patterns obtained from ejectors at 0.3 and 0.6 semispans. As mentioned before, particle concentration is expressed as percent of total deposit and plotted as a function of lateral distance from flight path. As expected, an increase in lateral spread and reduction in peak values associated with deposition from the more outboard ejector is noted. This occurs because particle trajectories become more nearly parallel to the ground and disperse more before impact as ejector location is moved outboard.

A marked similarity is noted between depositions from the different scale models. Although only mean-particle characteristics were scaled, and no attempt was made to scale the actual deposition patterns, the similarity between depositions indicates that deviations from mean-particle characteristics for different model scales is relatively uniform. This suggests the possibility of adjusting test-particle characteristics to be in agreement with full-scale droplet size distributions such that similar deposition patterns between small and full-scale tests are obtained.

## Visualization of Particle Trajectories

Early in this development effort, it was recognized that a method was needed to track the scaled test particles in the model-wake flow field. The ability to follow the motions of the particles in the wake was believed to be essential to evaluation of both particle transport mechanisms and methods for reducing particle entrainment in the wing-tip vortex flow.

A photographic technique has been developed over the past two years to visualize particle trajectories in the model wake. The technique is based on the fact that the trajectories of small particles released in an aircraft wake are generally confined to planes perpendicular to the flight path since longitudinal-flow velocities in the wake are small except for a region close to the vortex core. The technique utilizes a high intensity "light curtain" beamed across the model flight path to illuminate the particles, and trajectories are recorded by streak photography. The sketch and photographs shown in Figure 12 illustrate this trajectory-visualization technique. The sketch depicts a time sequence of a test run with the model at three successive positions as it passes through the facility test section. The three photographs show in sequence, from top to bottom, particle motion which has taken place in the light curtain in

the time which has elapsed when the model is at the three positions shown in the sketch. In the top photograph the model is seen passing through the light curtain, and particles -- in this case small glass beads -- which are being released from two ejectors under each wing are illuminated by the light. In the second photograph, the glass beads from the inboard ejector have almost deposited, their trajectories recorded as streaks on the photographic film, whereas those from the outboard ejector are being swept up by the rotating flow around the wing-tip vortex. In the bottom photograph beads from the inboard ejector have deposited, but most of those from the outboard ejector are clearly entrained in the wing-tip vortex. Normally, a strobe light is flashed the instant the model is in the light curtain and this records the model image on the final photograph which serves as a helpful frame of reference when viewing the trajectories. This technique was used to record the model image in the top photograph in this figure. Recently, this method to visualize particle trajectories has undergone a number of refinements to improve its sensitivity and enable tracking the smallest glass beads currently in use, most of which are under 100 microns in diameter. The glass beads used to make the trajectory photographs in Figure 12, for instance, are about 50 microns in size. The trajectory analyses made possible by such photographs are proving to be a sensitive diagnostic tool for evaluating the effectiveness of methods to reduce particle entrainment.

Analysis of Deposition

A computer program has been developed to analyze the scaled deposit data to provide a measure of uniformity of deposition over the treated field and an estimate of drift from the target area (ref. 8). Figure 13 illustrates program data requirements and typical output. Data requirements (upper figure) are single-ejector deposition median positions as functions of ejector position for three scaled particle sizes. In the case of liquid droplet simulation, tests are required with scaled particles corresponding to the smallest, mean, and largest droplet in the size spectrum of the particular full-scale nozzle that is being simulated. Of course, the more accurately the droplet size spectrum is known for the aircraft airspeed and nozzle orientation of interest (since droplet size is a function of both of these parameters), the more accurate will be the simulation. For the case of dry granular materials, the three scaled particles simply correspond to the smallest, mean, and largest seed or granule.

The program first develops a concentration distribution for each spanwise release point for which deposit data was entered (upper figure), by utilizing the expression for concentration:

$$C = Q \cdot \frac{dv}{d\delta} \cdot \frac{d\delta}{dy_G} ,$$

assuming a normal distribution of mass over the particle size spectrum. The individual concentration distributions are then summed to obtain the full single-swath deposition (lower left figure).

The uniformity and width of a single-swath deposition give little information with regard to overall field uniformity and optimum spacing of adjacent swaths. However, if a round-robin flight path is assumed and two adjacent swaths are overlapped, the effective swath width can be determined which corresponds to the most uniform overall deposition.

To determine optimum swath width, the program first splits the single swath along its centerline and positions the two halves of the deposition tip-to-tip. It then progressively moves the two halves closer, overlapping them (lower right figure), and at each step calculates the standard deviation and mean of the overall deposition. The ratio of these, the coefficient of variation, is monitored, and the swath spacing corresponding to the lowest value of this ratio is determined. This effective swath width is optimum from the standpoint that it corresponds to the most uniform deposition over the field.

The program also estimates amount of drift, defined here as that material entrained in the wing-tip vortex, by analyzing the deposit data from the outboard release points where vortex entrainment of smaller particles is occurring. By data interpolation the smallest particle which deposits without entrainment for each release point is determined. Assuming a normal mass distribution over the particle size spectrum, the relative mass made up of particles smaller than this is calculated for each release point, summed over all release points, and expressed as a percent of the total mass ejected. It is expected that this computer analysis will enable meaningful comparisons to be made between tests in the Vortex Facility and with full-scale field operations.

Model Size Constraints

Theoretical analysis and vortex-trajectory experiments have aided in establishing boundaries of the facility test envelope for models of different scale (ref. 9). When an aircraft is in close ground proximity, the main effect of the ground on the vortex system is to restrict its normal descent and to cause a rapid outboard movement of the system laterally over the ground. An interesting phenomenon, discussed in reference 3, is the tendency for the vortex system to migrate upward or rebound away from the ground as it moves laterally outboard. This has been explained as resulting from the viscous "scrubbing" action of the vortex on the ground. Vortex rebound is observed in Vortex Facility tests, but at relatively large distances behind the airplane the rebound is believed to be in part due to interference resulting from proximity of the test-section side walls. In order for facility deposition data to be valid, the test particles must be on the ground before facility walls significantly distort the model aircraft wake. The objective of the vortex trajectory experiments was to distinguish between vortex rebound and the nearly identical side wall effects.

A comparison of vortex trajectories in ground effect from the three models previously discussed in the scaling study is shown in Figure 14. Time variation of vortex core position is determined from photographs similar to those in Figure 4 and is plotted as a function of distance behind the aircraft, in wing semispans (indicated by the numbered ticks on the data curves). Vertical and horizontal scales are height above the ground plane and lateral distance from the flight path, respectively, in wing semispans. A sketch representing a scaled front-view of the models is

included as a graphic aid. Distance of test section walls from flight path for each of the models is also indicated on the figure.

For the smallest model, the slight vortex rebound that occurs about 30 semispans downstream is attributed to the vortex-bounce phenomena, but the rapid upward movement that is seen about 75 semispans downstream is caused by test section walls. Points at which wall effects occur for the two larger models are determined by noting the points at which their trajectories diverge from that of the smallest model. The vortex trajectories shown in Figure 14 indicate this point occurs about 52 semispans downstream for the intermediate sized model and about 28 semispans downstream for the largest model.

This vortex trajectory data was used in conjunction with theoretical calculations to determine the time required (or alternately the distance downstream from the aircraft) for particles to deposit on the ground for a range of particle sizes and aircraft altitudes and lift coefficients, for the three models. A validation of the numerical aircraft wake flow field used in these calculations was obtained by comparison of calculated and measured vortex trajectories. These experiments have defined the test envelope consisting of model size, particle characteristics, and test conditions, for valid aerial applications tests in the Vortex Facility.

## Recent Deposition Studies

### Typical Spray Deposition

Spray deposition patterns from a one-tenth scale model of a representative low-wing agricultural monoplane have been measured in recent tests. In these tests dispersal from forty nozzles on a full-length boom (extends full-length of the wing) was simulated in the computer analysis of data. Glass sphere microbeads that scaled to represent the minimum, mean, and maximum size water droplets from a typical nozzle designed for improved drift control were used in these tests. Model altitude corresponded to a boom height above the ground of about 10 feet and model attitude corresponded to a lift condition of near maximum gross weight.

Data analysis of this test case indicates an optimum effective swath width of about two-and one-quarter semispans with nearly 20 percent of the spray potentially drifting because of entrainment in the wing-tip vortex. A well-known method of reducing spray drift due to entrainment is to reduce the length of the spray boom, eliminating release of drops near the wing tip. In order to investigate the effectiveness of this method the test case just described was also analyzed assuming various boom lengths. The results are presented in Figure 15 in which reduction in drift and optimum effective swath width due to reducing boom length are plotted as a function of boom reduction. This analysis indicates that reducing boom length is an effective means to reduce drift with greater than an 80-percent reduction in drift realized by reducing boom length 20 percent. A penalty is incurred, however, in that optimum swath width is reduced about 12 percent for the same reduction in boom length. It is interesting to note that no change in swath width occurs for the first 5-percent reduction in boom length. The explanation for this result is that all of the spray from the last three nozzles is entrained in the wing-tip vortex. Since none of the material is depositing, eliminating these three nozzles has no effect on swath width.

### Wake Modification

A number of methods of aerodynamic-wake modifications have evolved through efforts of researchers to minimize the upset hazard associated with wake vortices behind large jet transport aircraft. These methods alter wake properties through use of aerodynamic-flow mechanisms (tailoring spanwise circulation, or injecting turbulence for example). Several candidate concepts for modifying wakes of agricultural airplanes are shown in Figure 16. Use of some of these concepts may improve drift control because they are known to attenuate vortex flow at the wing tip (splines (ref. 10) or winglets (ref. 11), for example), while use of some may increase effective swath width because they enhance spanwise flow under the wing (span-loading alteration, for example). Some of these wing-tip concepts were originally developed for purposes other than wake modification. Winglets, for instance, were originally designed for induced drag reduction. More recently, wing-tip sails, developed at the Cranfield Institute of Technology, England, have been proposed for performance gain as well as improved drift control for agricultural aircraft.

Exploratory tests have been conducted with several of the illustrated concepts. Winglets were identified early as a concept meriting evaluation because they are known to cause a vertical diffusion of the tip vortex flow just downstream of the wingtip (ref. 11). Early tests, reported in reference 3, indicate that in ground effect winglets can displace the centroid of vorticity upward, resulting in vortex roll-up near the tip of the winglet. The vortex, once formed, moves laterally over the ground at a height above that of the baseline vortex. These tests further indicated that this vortex upward shift may reduce particle entrainment, because a reduction in lateral displacement of particle deposit was observed

More recently, winglets have been tested on the 1/10-scale low-wing monoplane for which baseline spray deposition data was previously presented. Typical effects of winglets on the vortex, presented as vortex trajectory plots in Figure 17, are similar to effects seen in the earlier tests. Vortex roll-up is displaced upward a distance greater than half the winglet span, and the vortex trajectory with winglets on remains above the baseline for large distances downstream.

Recent full-scale wind tunnel tests on this winglet configuration have identified potentially serious problems in some areas of stability and control when the winglets are canted outward (ref. 12). However, these wind tunnel tests as well as unpublished results of recent flight simulator studies at Langley have indicated that the adverse winglet effects on stability and control are alleviated when the winglets are canted inward 10 degrees. The vortex trajectory plots in Figure 17 show that the desired effect of winglets on vortex roll-up position and transport are not diminished

when the winglets are canted inward 10 degrees.

In order for winglets to be effective in raising vortex roll-up position they must carry substantial aerodynamic lift (winglet incidence is set to produce inwardly directed aerodynamic lift on the winglet). This is illustrated in Figure 18 in which vortex trajectory plots are presented for winglet incidence angles ranging from 0 to 7.5 degrees. At winglet incidence angles of 5 and 7.5 degrees substantial vortex upward displacement is seen, but at incidence of 0 degrees the initial formation of an additional vortex at the wing tip, although it quickly merges with the winglet vortex, nevertheless inhibits the upward displacement of the final vortex system. The important point to recognize is that in order to be effective and practical the configuration must be carefully tailored in terms of its effect on both the wake and aircraft flight characteristics.

In considering the possible benefits on spray-drop entrainment to be derived from displacing the wing-tip vortex upward, an important consideration is the degree to which the flow upwash at the wing tip, near the spray nozzles, has been reduced. Reductions in laser-measured vertical velocity profiles at the level of the wingtip due to winglets for ranges of winglet incidence and cant angles are presented in Figure 19. These flow velocity profiles indicate substantial velocity reductions at the wing tip with either inward- or outward-canted winglets as long as a reasonably large winglet incidence is maintained.

Typical effects of this winglet configuration on entrainment of particles released from ejectors near the wingtip are illustrated in the particle trajectory photographs in Figure 20. In these photographs glass microbeads that scale to 477-micron-diameter water drops have been released from ejectors at spanwise positions of 0.60 and 0.80 semispans. Winglet cant and incidence are -10 degrees (inward) and 5 degrees, respectively. The particle trajectories in these photographs indicate that with winglets off about half of the material released from the 0.8 semispan position is entrained in the vortex, whereas with winglets installed very little entrainment of this material occurs.

In order to obtain some quantitative assessment of winglet drift-control effectiveness, deposition data with winglets installed was analyzed assuming a range of boom lengths from 1.0 to 0.8 semispans and the "drift profile" of this configuration compared with the typical spray deposition case discussed previously. This comparison is presented in Figure 21 as percent reduction in drift (from that realized with a full-length boom) plotted against the corresponding reduction in optimum effective swath width. These data indicate that for a given optimum swath width this winglet configuration would improve drift control over the range of boom lengths presented, with the greatest improvement realized with a near full-length boom.

It is not certain, of course, that these winglet effects will prove significant in actual full-scale field operations, where a number of meteorological factors do play significant roles. Flight deposition tests will be required to resolve such uncertainties. However, results to date are promising because they demonstrate that wake properties can be tailored aerodynamically to produce desirable changes in deposition characteristics.

## Concluding Remarks

As a key element in the NASA aerial applications technology effort, test methods have been developed over the past three years at the Langley Vortex Research Facility to simulate and measure deposition patterns of aerially-applied sprays and granular materials by means of tests with small-scale models of agricultural aircraft and dynamically-scaled test particles. Particle trajectory scaling laws which apply to scaling both liquid droplets and agricultural granulars have been developed and experimentally validated by facility tests. Experimental techniques have been developed to disperse the scaled test particles from model aircraft, photographically measure particle trajectories in the model wake, and collect and analyze the deposition data to provide quantitative comparisons of pattern uniformity, effective swath width and drift characteristics. Exploratory tests with winglets have demonstrated that wake properties can be tailored aerodynamically to produce desirable effects on deposition and drift characteristics. It is believed that these experimental and analytical methods provide the necessary research tools to conduct aerial applications studies under controlled conditions heretofore unavailable, and demonstrate the potential of the Vortex Research Facility in the NASA Aerial Applications Program.

## References


1. Akesson, Norman B.; and Yates, Westley E.: The Use of Aircraft in Agriculture. Food and Agriculture Organization of the United Nations (FAO) Agricultural Development Paper No. 94, 1974.

2. Holmes, Bruce J.; Morris, Dana K.; and Razak, Kenneth: Data and Analysis Procedures for Improved Aerial Applications Mission Performance. ASAE AA79-001, Proceedings of 1979 ASAE/NAAA Jointly Sponsored Technical Session on Agricultural Aviation Research, December 10-13, 1979.

3. Jordan, Frank L., Jr.; McLemore, H. Clyde; and Bragg, Michael B.: Status of Aerial Applications Research in the Langley Vortex Research Facility and the Langley Full-Scale Wind Tunnel. NASA TM-78760, 1978.

4. Patterson, James C., Jr.; and Jordan, Frank L., Jr.: A Static Air Flow Visualization Method to Obtain a Time History of the Lift-Induced Vortex and Circulation. NASA TMX-72769, 1975.

5. Gartrell, Luther R.; and Jordan, Frank L., Jr.: Demonstration of Rapid-Scan Two-Dimensional Laser Velocimetry in the Langley Vortex Research Facility for Research in Aerial Applications. NASA TM-74081, 1977.

6. Rhodes, David B.: Optical Scanning System for Laser Velocimeters. Proceedings of the Society of Photo-Optical Instrumentation Engineers, Vol. 84, Laser Scanning Components and Techniques, 1976, pp. 78-84.

7. Ormsbee, A. I.; and Bragg, M. B.: Trajectory Scaling Laws for a Particle Injected into the Wake of an Aircraft. Institute of Aviation, Aviation Research Lab, University of Illinois, Technical Report ARL-78-1.

8. Holzhei, Donald E.: Development of the Simulation of Agricultural Particles in the Langley Vortex Research Facility. To be published as a NASA Technical Memorandum.

9. Ormsbee, A. I.; Bragg, M. B.; and Maughmer, Mark D.: The Development of Methods for Predicting and Measuring Distribution Patterns of Aerial Sprays. Institute of Aviation, Aviation Research Lab, University of Illinois, Technical Report ARL-79-1.

10. Patterson, J. C., Jr.; Hastings, E. C., Jr.; and Jordan, Frank L., Jr.: Ground Development and Flight Correlation of the Vortex Attenuating Spline Device. Proceedings of Symposium on Wake Vortex Minimization. NASA SP-409 pp. 271-303.

11. Whitcomb, Richard T.: A Design Approach and Selected Wind-Tunnel Results at High Subsonic Speeds for Wing-Tip Mounted Winglets. NASA TND-8260, July 1976.

12. Johnson, Joseph L., Jr.; McLemore, H. Clyde; White, Richard L.; and Jordan Frank L., Jr.: Full Scale Wind-Tunnel Investigation of an Ayres S2R-800 Thrush Agricultural Airplane. SAE Technical Paper 790618, Proceedings of 1979 SAE Business Aircraft Meeting and Exposition, April 3-6, 1979.

Figure 1.- Example of spray-wake interaction.

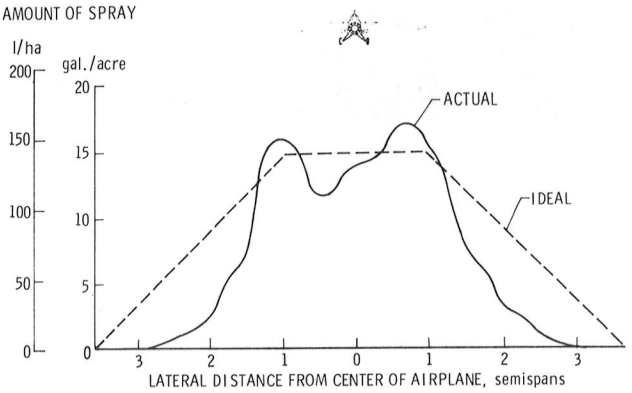


Figure 2.- Typical effects of interactions on deposition pattern.

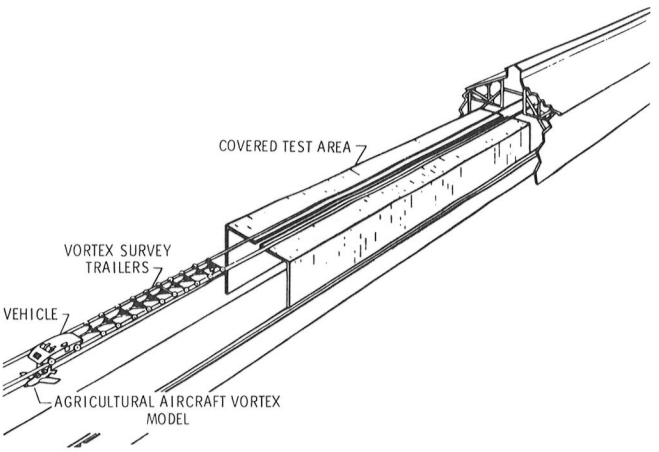


Figure 3.- Sketch of the Langley Vortex Research Facility.

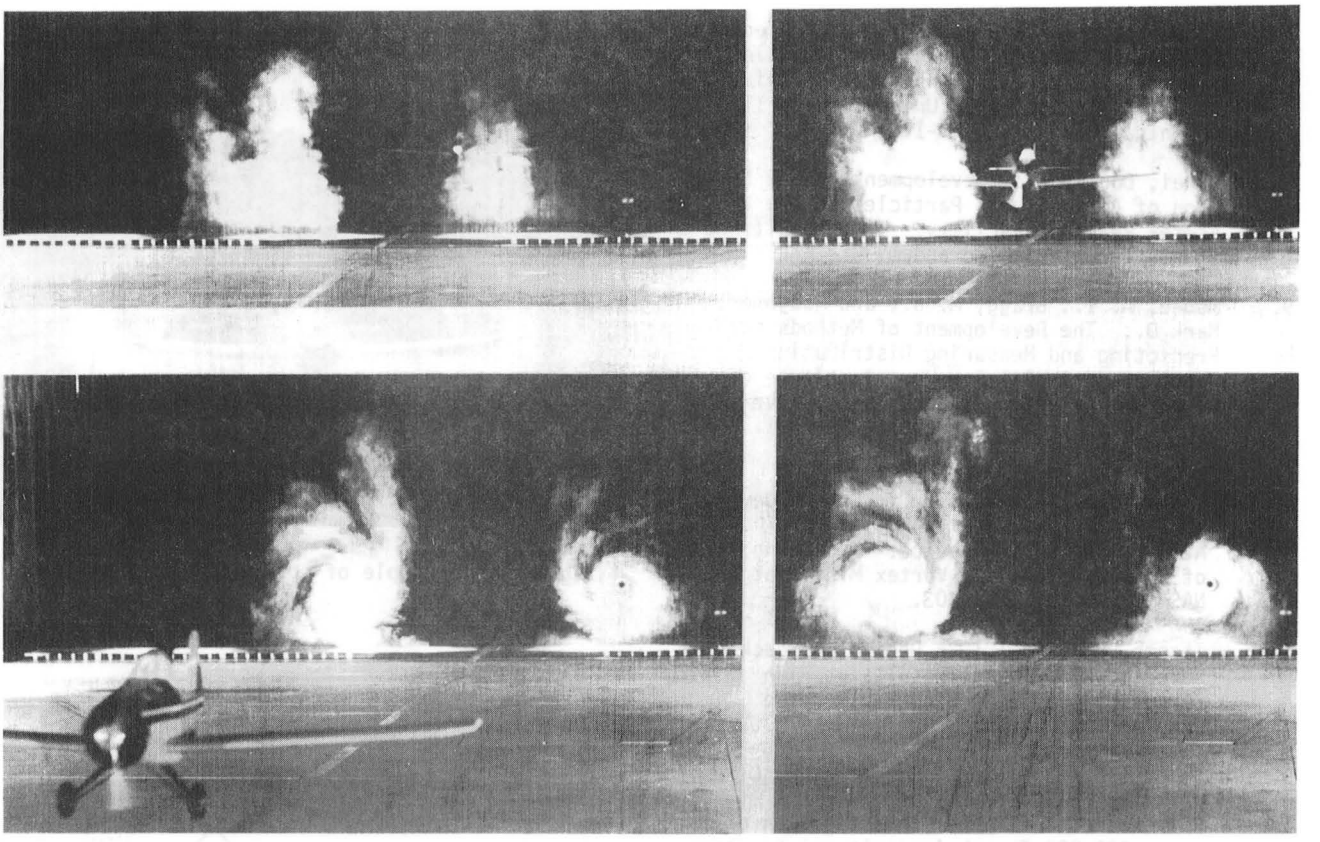

Figure 4.- Flow visualization of model aircraft wake-vortex system in ground effect.

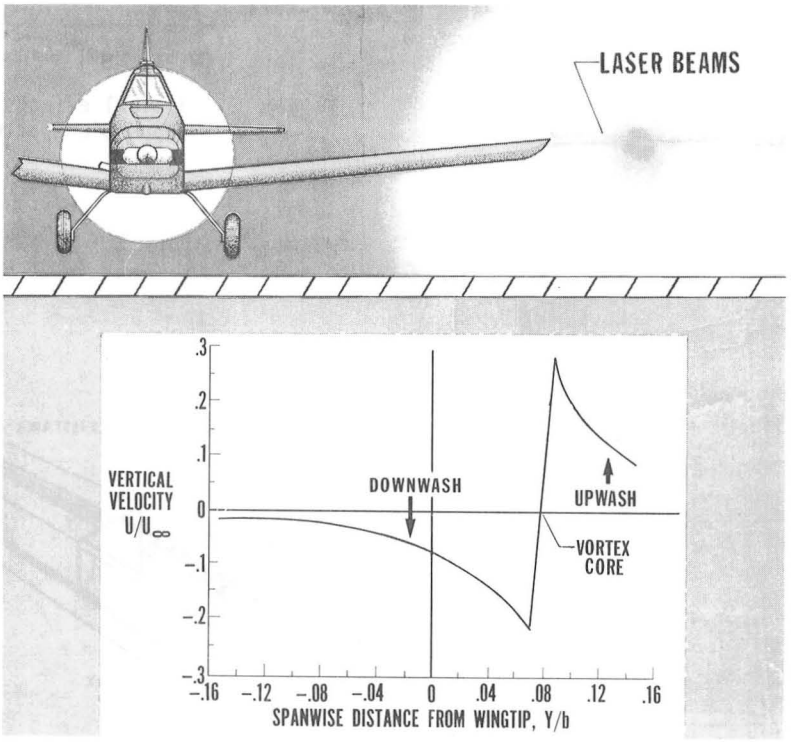


Figure 5.- Laser-doppler velocimeter measurement of wake vortices.

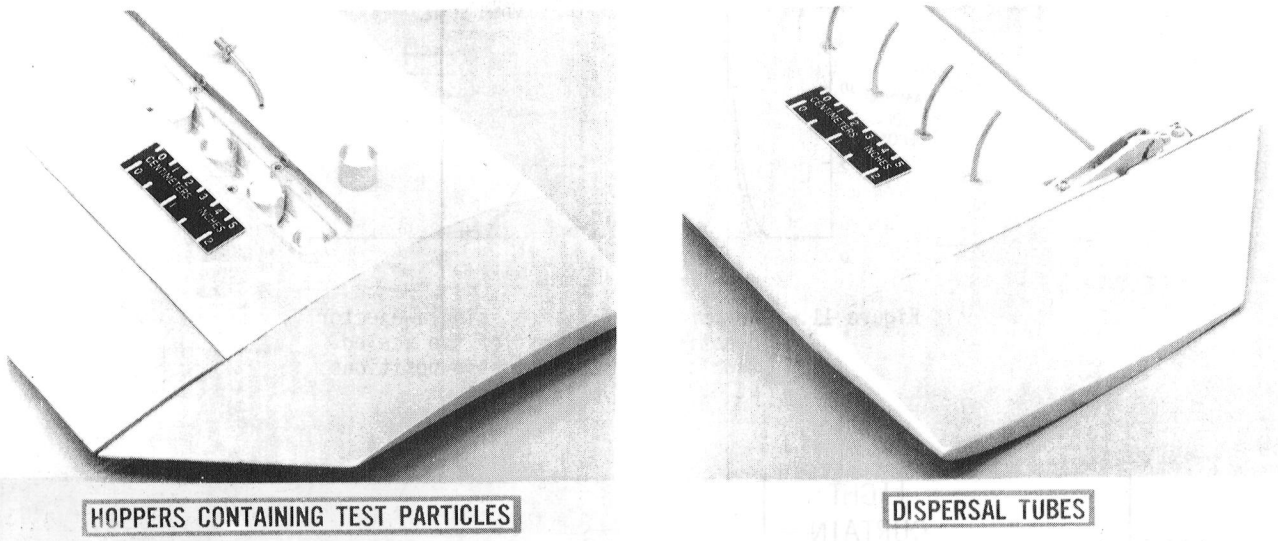


Figure 6.- Particle dispersal system installed in wing of model aircraft.

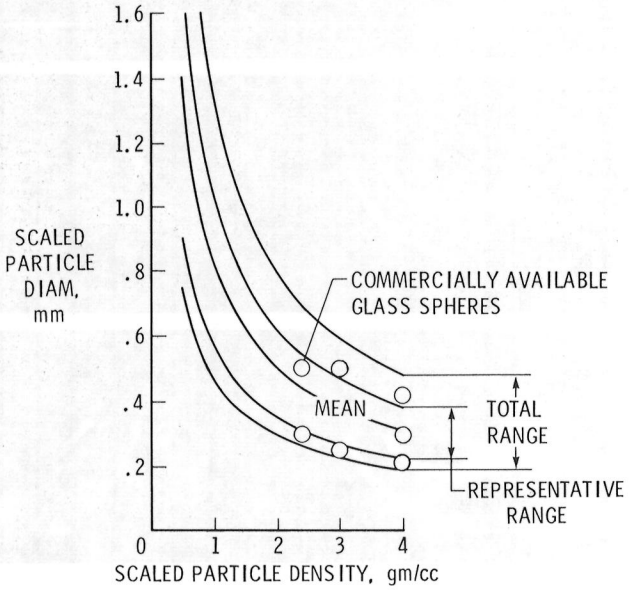


Figure 7.- Wheat seeds scaled to one-tenth.

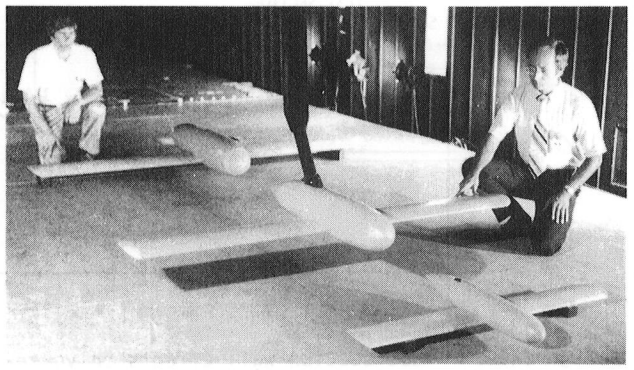

Figure 8.- Unpowered experimental model aircraft used in the scaling law validation tests.

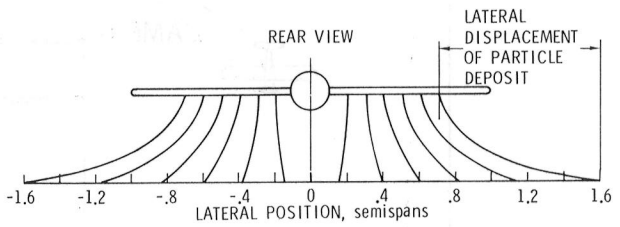


Figure 9.- Median-deposit trajectories for the scaling law validation.

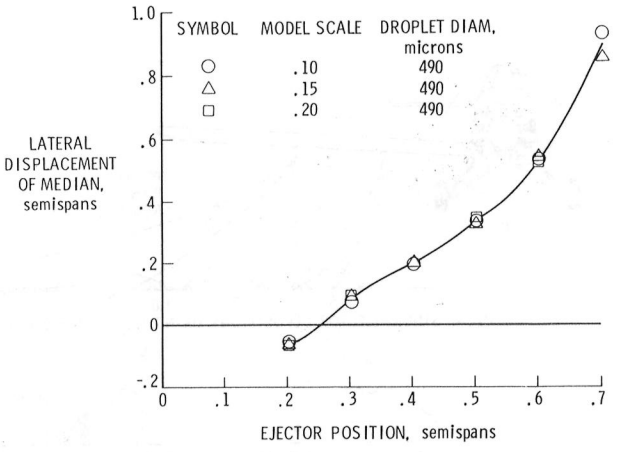


Figure 10.- Comparison of lateral displacement of deposition medians for the scaled models.

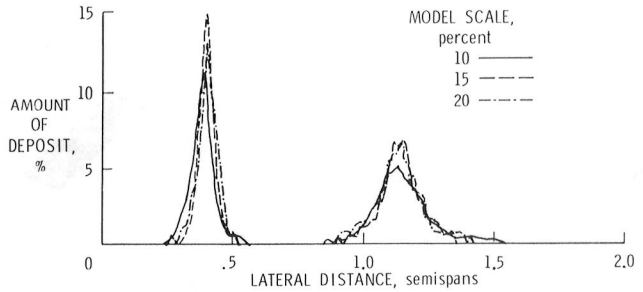


Figure 11.- Comparison of typical single-ejector deposition patterns for the scaled models. Ejector spanwise positions at 0.3 and 0.6 semispans.

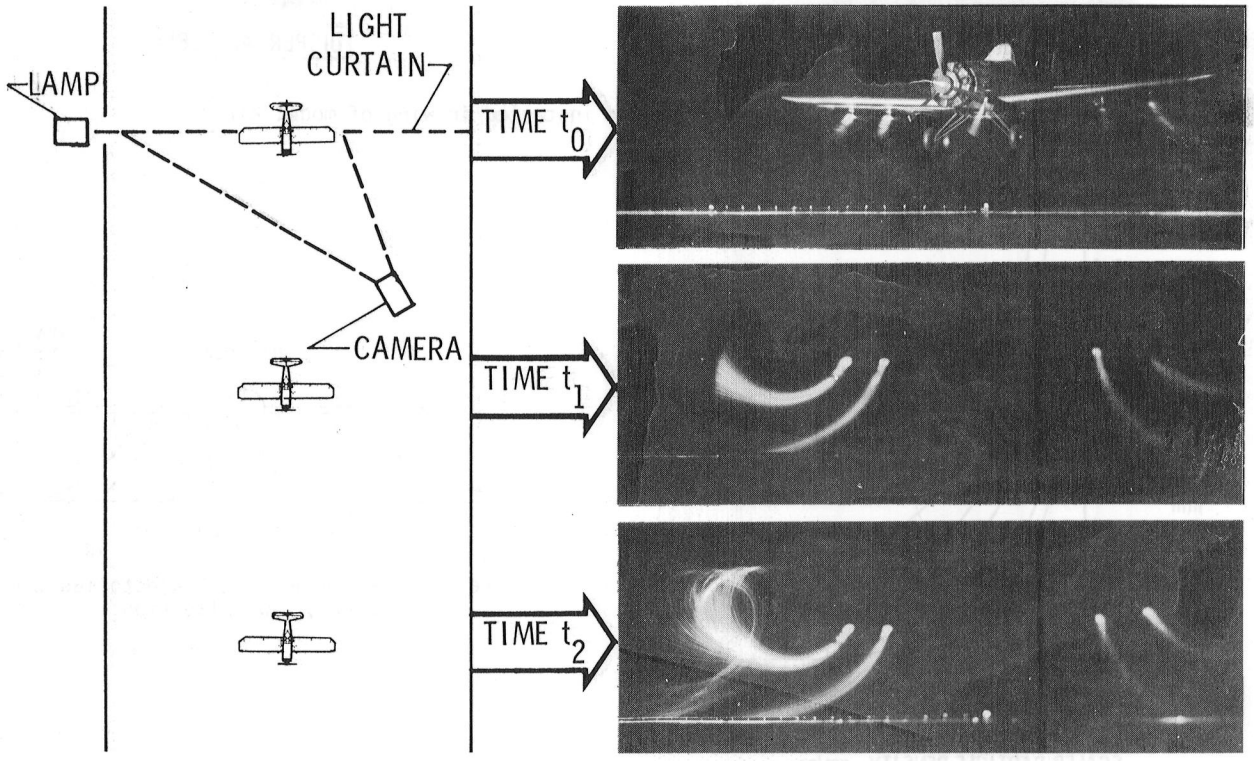


Figure 12.- Visualization of particle trajectories.

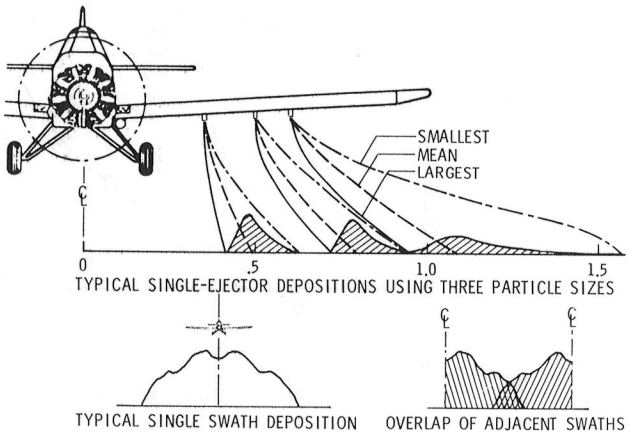


Figure 13.- Computer analysis of particle deposition data.

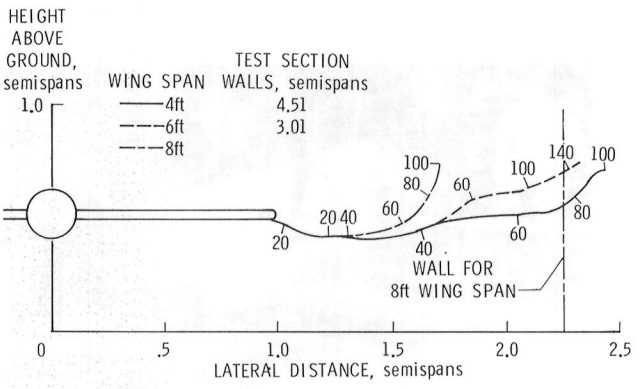


Figure 14.- Test-section wall effects on vortex lateral transport in ground effect for scaled models. Numbered ticks on curves indicate downstream distance from model in wing semispans.

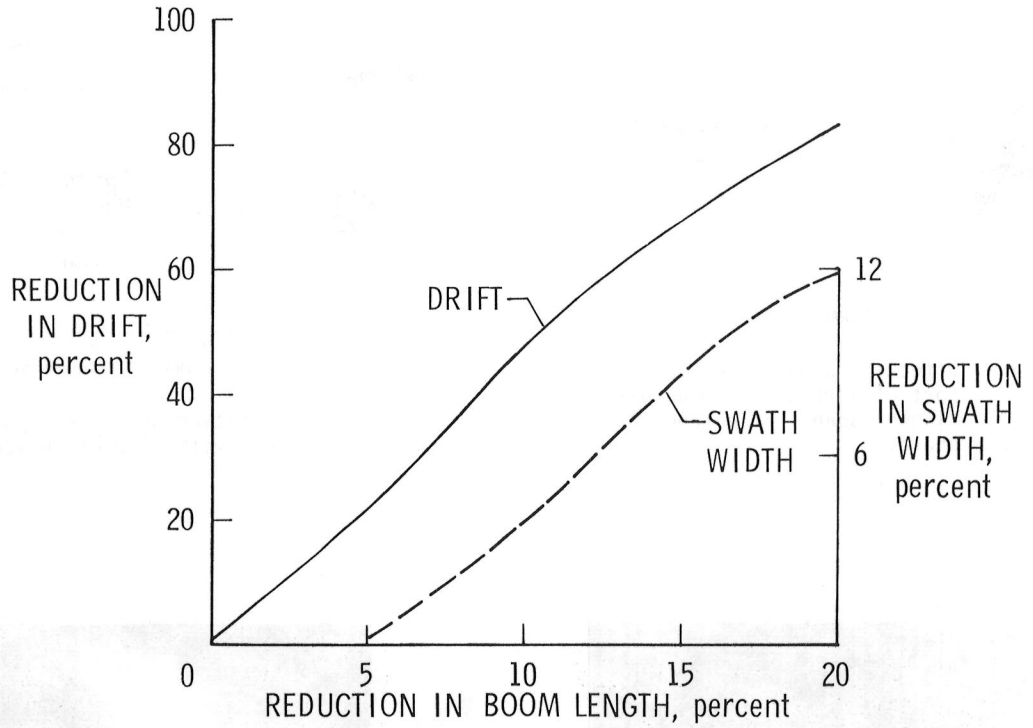


Figure 15.- Effect of boom length on drift and swath width relative to values with full-length boom.

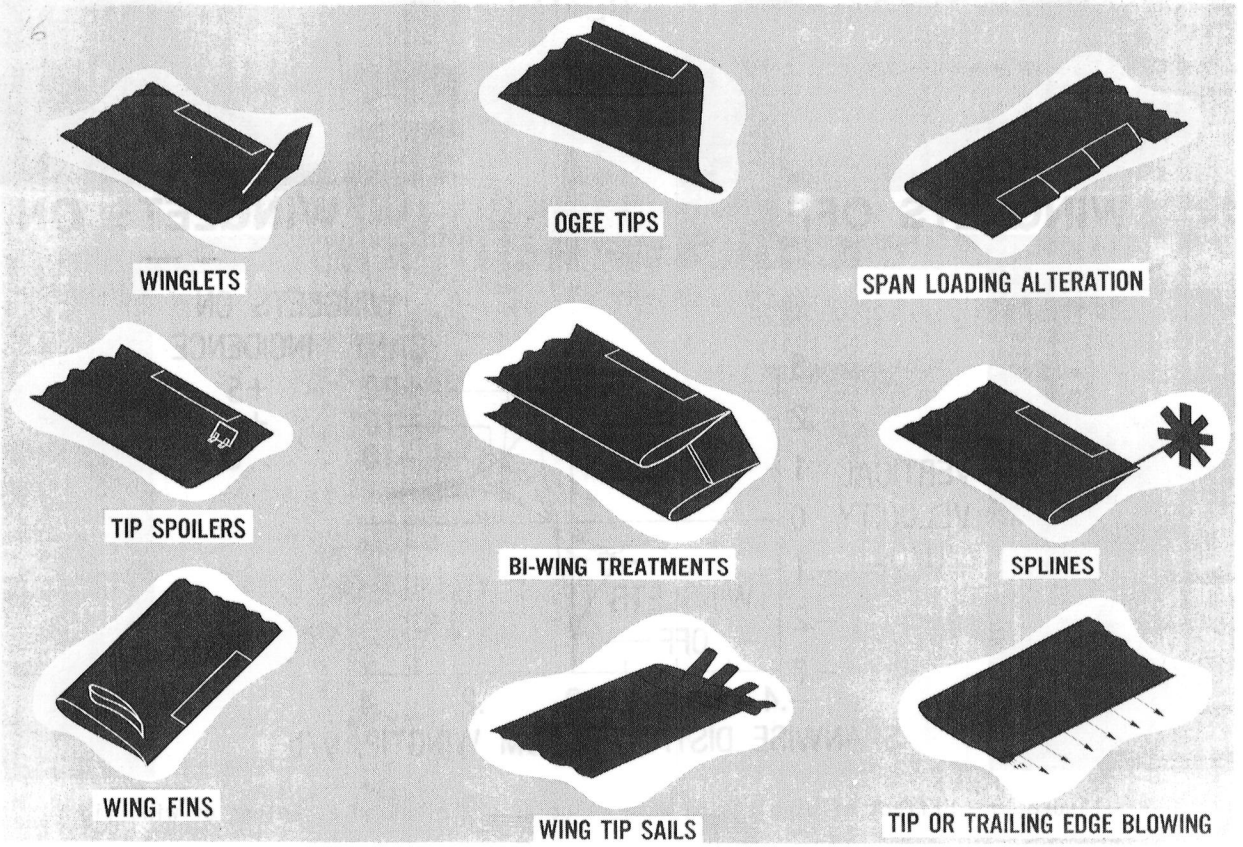


Figure 16.- Candidate wing treatments for wake modification of agricultural airplanes.

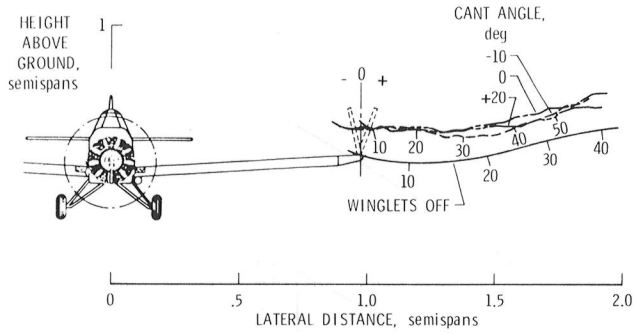


Figure 17.- Effect of winglets on lateral transport of vortex in ground effect. Winglet span = 67 percent of wing chord.

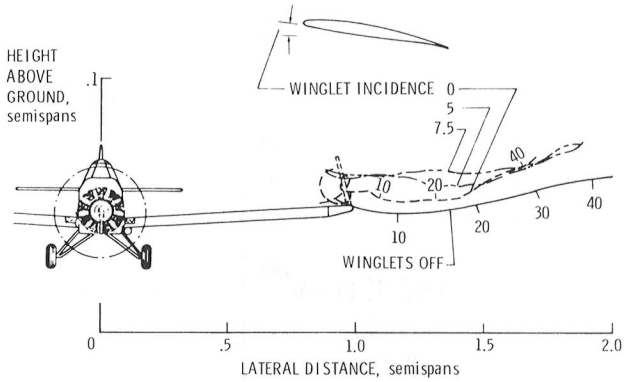


Figure 18.- Variation of vortex upward displacement with winglet incidence angle.

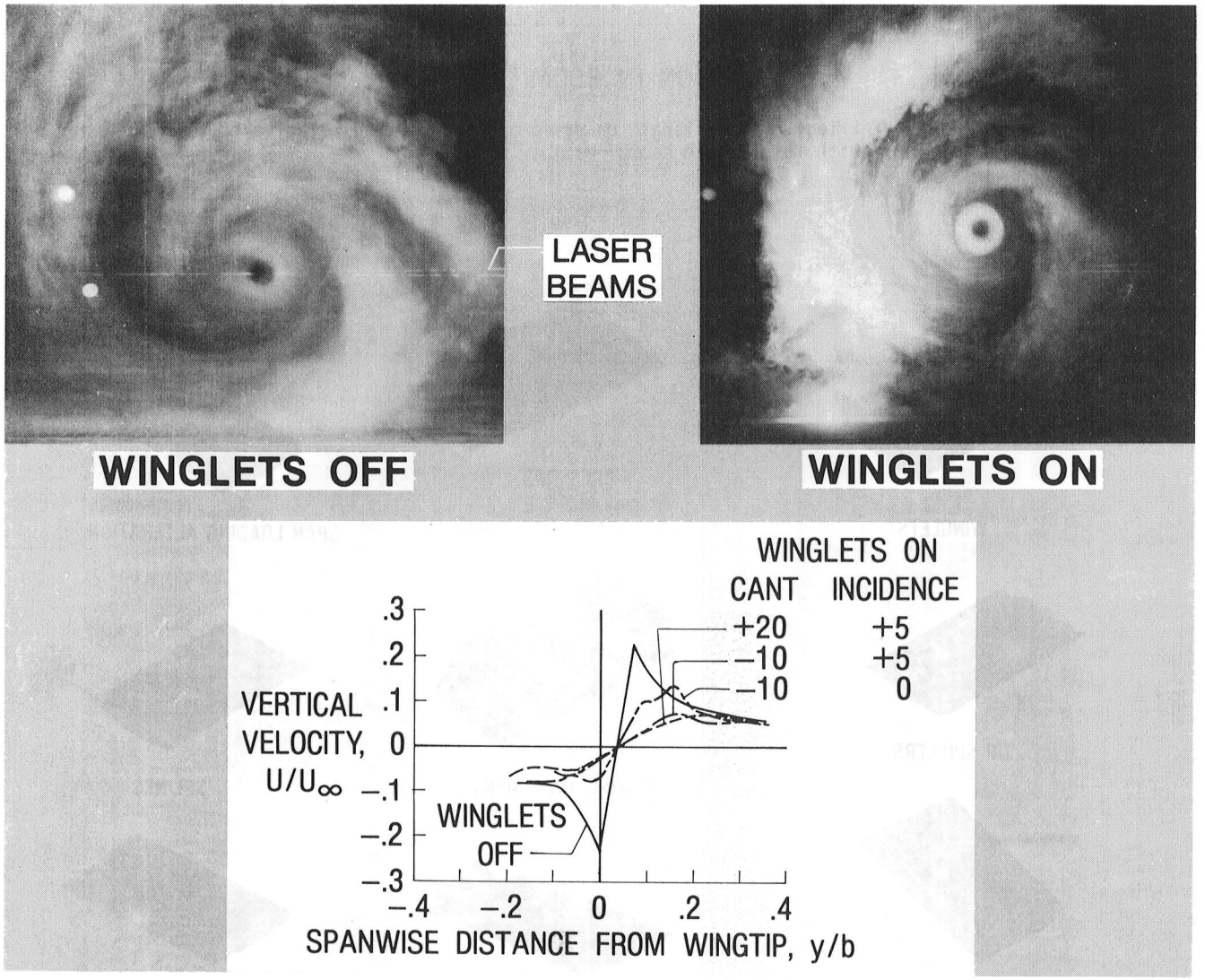


Figure 19.- Effect of winglets on wake velocity distribution at height of wing tip.

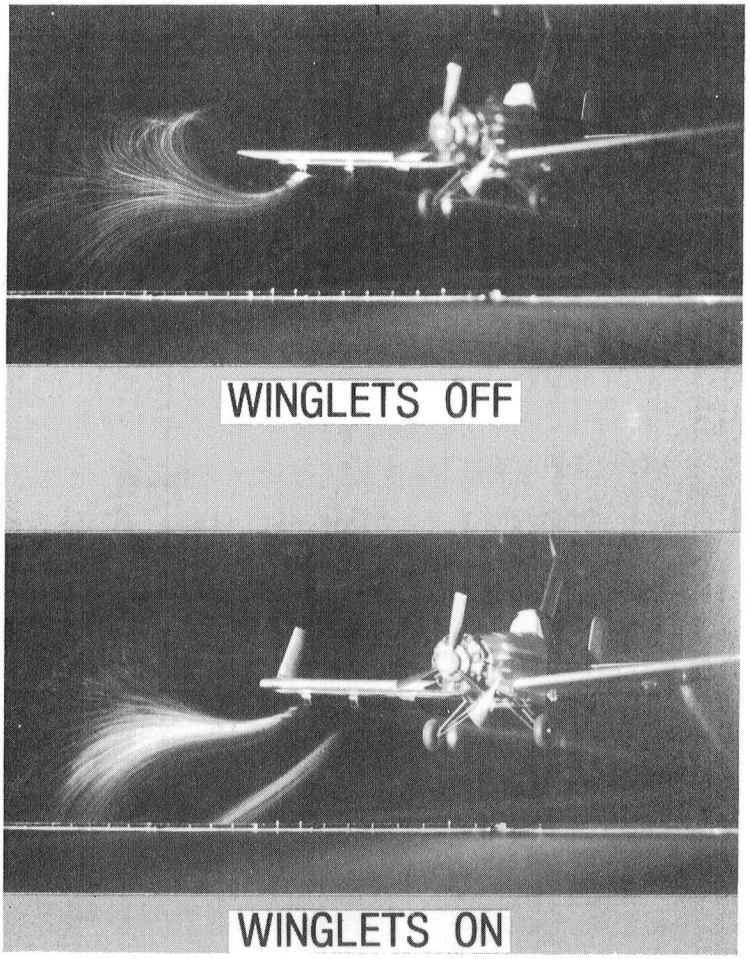


Figure 20.- Visualization of effects of winglets on entrainment of particles in vortex.

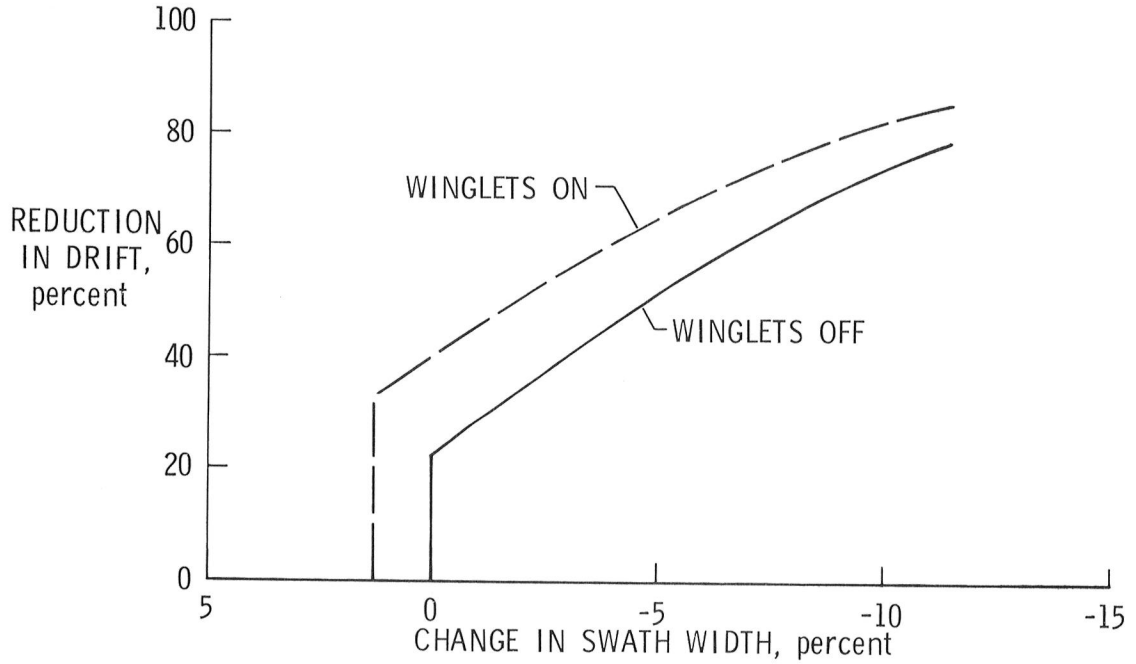


Figure 21.- Effect of winglets on drift and swath width for range of boom lengths from full to 80-percent semispan. Negative change in swath width indicates reduction.

| 1. Report No. | 2. Government Accession No. | 3. Recipient's Catalog No. |
|---|---|---|
| NASA TM-81805 | | |

| 4. Title and Subtitle | 5. Report Date |
|---|---|
| Development of Test Methods for Scale Model Simulation of Aerial Applications in the NASA Langley Vortex Research Facility | April 1980 |
| | 6. Performing Organization Code |
| 7. Author(s) | 8. Performing Organization Report No. |
| Frank L. Jordan, Jr. | |
| 9. Performing Organization Name and Address | 10. Work Unit No. |
| NASA Langley Research Center<br>Hampton, VA 23665 | 505-41-83-01 |
| | 11. Contract or Grant No. |
| | 13. Type of Report and Period Covered |
| 12. Sponsoring Agency Name and Address | Technical Memorandum |
| National Aeronautics and Space Administration<br>Washington, D.C. 20546 | 14. Army Project No. |

15. Supplementary Notes

This paper was previously presented at the AIAA 11th Aerodynamic Testing Conference, March 18-20, 1980, Colorado Springs, Colorado

16. Abstract

The Langley Research Center of the National Aeronautics and Space Administration is currently engaged in basic research to improve aerial applications technology. As a key part of this program, methods have been developed at the Langley Vortex Research Facility to simulate and measure deposition patterns of aerially-applied sprays and granular materials by means of tests with small-scale models of agricultural aircraft and dynamically-scaled test particles. Interactions between the aircraft wake and the dispersed particles are being studied with the objective of modifying wake characteristics and dispersal techniques to increase swath width, improve deposition pattern uniformity, and minimize drift. This paper describes the particle scaling analysis, test methods for particle dispersal from the model aircraft, visualization of particle trajectories, and measurement and computer analysis of test deposition patterns. An experimental validation of the scaling analysis and test results that indicate improved control of chemical drift by use of winglets, are presented to demonstrate test methods.

| 17. Key Words (Suggested by Author(s)) | 18. Distribution Statement |
|---|---|
| Aerial Application, Agricultural Aircraft, Scale Model Test Methods, Wake Vortex, Pesticide Drift, Spray Deposition | Unclassified, Unlimited<br><br>STAR Category 01 |

| 19. Security Classif. (of this report) | 20. Security Classif. (of this page) | 21. No. of Pages | 22. Price* |
|---|---|---|---|
| Unclassified | Unclassified | 15 | $4.00 |

*For sale by the National Technical Information Service, Springfield, Virginia 22161